

Supplementary Information

**Versatile control of superconducting transition temperature in anti-ThCr₂Si₂-
type Y₂O₂Bi via H, Li, or F doping**

Kyohei Terakado,^a Hideyuki Kawasoko,^a and Tomoteru Fukumura^{*a,b}

^a*Department of Chemistry, Graduate School of Science, Tohoku University, Sendai 980-8578, Japan*

^b*Advanced Institute for Materials Research and Core Research Cluster (WPI-AIMR), Tohoku University, Sendai 980-8577, Japan*

* tomoteru.fukumura.e4@tohoku.ac.jp

Table S1 Molar ratio of (a) Y, Bi, and F for $Y_2(O,F)_2Bi$ and (b) Y, Bi, and Li for $Y_2O_2Bi:Li$ measured by ICP-MS and IC.

(a)				
Nominal composition	label	Y	Bi	F
$Y_2O_{1.5}Bi_{1.5}$	$x_F = 0$	2.00	1.04	0.00
$Y_2O_{1.4}F_{0.1}Bi_{1.5}$	$x_F = 0.1$	2.00	0.99	0.15
$Y_2O_{1.4}F_{0.2}Bi_{1.5}$	$x_F = 0.2$	2.00	1.00	0.26
$Y_2O_{1.4}F_{0.3}Bi_{1.5}$	$x_F = 0.3$	2.00	1.03	0.31

(b)				
Nominal composition	label	Y	Bi	Li
$Y_2O_{1.5}Bi_{1.0}$	$x_{Li} = 0$	2.00	1.00	0.00
$Y_2O_{1.5}Bi_{1.0} + (LiO_{0.5})_{0.5}$	$x_{Li} = 0.5$	2.00	1.01	0.48
$Y_2O_{1.5}Bi_{1.0} + (LiO_{0.5})_{1.0}$	$x_{Li} = 1.0$	2.00	1.00	1.00
$Y_2O_{1.5}Bi_{1.0} + (LiO_{0.5})_{1.5}$	$x_{Li} = 1.5$	2.00	0.96	1.32

Table S2 Summary of crystal structural data and superconducting transition temperature (T_c) for (a) $Y_2(O,H)_2Bi$, (b) $Y_2(O,F)_2Bi$, and (c) $Y_2O_2Bi:Li$ (R_{wp} : R -factor, R_e : expected R -factor, S : goodness-of-fit indicator).

(a)

Nominal composition	label	a (Å)	c (Å)	c/a	R_{wp}	R_e	S	T_c (K)
$Y_2O_{1.5}Bi_{1.5}$	$x_H = 0$	3.8746	13.272	3.4254	2.207	1.438	1.535	2.14
$Y_2O_{1.5}Bi_{1.5} + (Ca_{0.5}H)_{0.4}$	$x_H = 0.4$	3.8718	13.282	3.4304	2.782	1.499	1.855	2.20
$Y_2O_{1.5}Bi_{1.5} + (Ca_{0.5}H)_{1.0}$	$x_H = 1.0$	3.8729	13.290	3.4316	3.529	1.512	2.334	2.21

(b)

Nominal composition	label	a (Å)	c (Å)	c/a	R_{wp}	R_e	S	T_c (K)
$Y_2O_{1.5}Bi_{1.5}$	$x_F = 0$	3.8746	13.272	3.4254	2.207	1.438	1.535	2.14
$Y_2O_{1.4}F_{0.1}Bi_{1.5}$	$x_F = 0.1$	3.8714	13.234	3.4184	3.248	1.568	2.071	1.95
$Y_2O_{1.4}F_{0.2}Bi_{1.5}$	$x_F = 0.2$	3.8721	13.217	3.4133	2.607	1.533	1.701	1.90
$Y_2O_{1.4}F_{0.3}Bi_{1.5}$	$x_F = 0.3$	3.8742	13.104	3.3823	3.043	1.559	1.952	-

(c)

Nominal composition	label	a (Å)	c (Å)	c/a	R_{wp}	R_e	S	T_c (K)
$Y_2O_{1.5}Bi_{1.0}$	$x_{Li} = 0$	3.8712	13.254	3.4238	2.288	1.553	1.473	2.19
$Y_2O_{1.5}Bi_{1.0} + (LiO_{0.5})_{0.5}$	$x_{Li} = 0.5$	3.8720	13.262	3.4251	2.195	1.569	1.400	2.24
$Y_2O_{1.5}Bi_{1.0} + (LiO_{0.5})_{1.0}$	$x_{Li} = 1.0$	3.8709	13.265	3.4269	2.326	1.524	1.527	2.25
$Y_2O_{1.5}Bi_{1.0} + (LiO_{0.5})_{1.5}$	$x_{Li} = 1.5$	3.8716	13.268	3.4270	2.378	1.525	1.559	2.27

Chemical composition analysis of $Y_2(O,H)_2Bi$ by SEM-EDX

The inner wall of quartz tube was considerably covered by yellowish deposit after the synthesis of $Y_2(O,H)_2Bi$ ($x_H = 1.0$) (inset of Fig. S1a). Figure S1a shows EDX spectrum of the inner wall after the synthesis of $Y_2(O,H)_2Bi$ ($x_H = 1.0$), representing that the specimen was composed of Ca in addition to Si and O from the quartz tube. In scanning electron micrograph of the $Y_2(O,H)_2Bi$ ($x_H = 1.0$), three kinds of crystal grains were observed with color of gray, black, and white (Fig. S1b). In EDX mapping images (Figs. S1c–S1e), Y, O, and Bi signals were almost homogeneously distributed in the gray area, corresponding to Y_2O_2Bi phase. In addition, intense Y and Bi signals were observed in the black and white area, indicating the presence of Y_2O_3 and Bi impurity phase, respectively. Intense Ca signal was observed in the white area where intense Bi was also observed. EDX spectra in selected small areas show that Ca was only detected in the Bi-rich white area (1, 2, 3 in Fig. S1b), indicating that the presence of Y-O-Bi, Y-O, and Bi-Ca phases (Fig. S2), respectively, corresponding to Y_2O_2Bi , Y_2O_3 , and Bi (mixed with Ca) phases evaluated from the Rietveld analysis (Fig. 1 and Table S2). Accordingly, Ca was not incorporated in Y_2O_2Bi phase, but was incorporated in Bi impurity phase and evaporated on the quartz tube. These XRD and EDX results of $Y_2(O,H)_2Bi$ indicate that CaH_2 served as H dopant for Y_2O_2Bi .

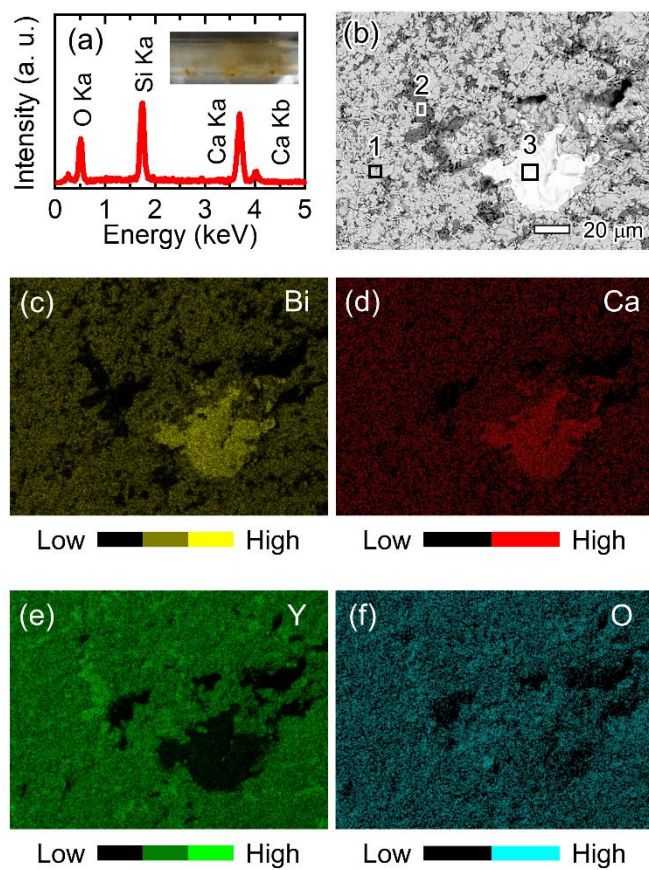


Figure S1 (a) Energy dispersive x-ray (EDX) spectrum for inner wall of quartz tube after synthesis of $Y_2(O,H)_2Bi$ ($x_H = 1.0$). Inset shows the photograph of the quartz tube. (b) Scanning electron micrograph of $Y_2(O,H)_2Bi$ ($x_H = 1.0$). The EDX mappings for (c) Bi, (d) Ca, (e) Y, and (f) O.

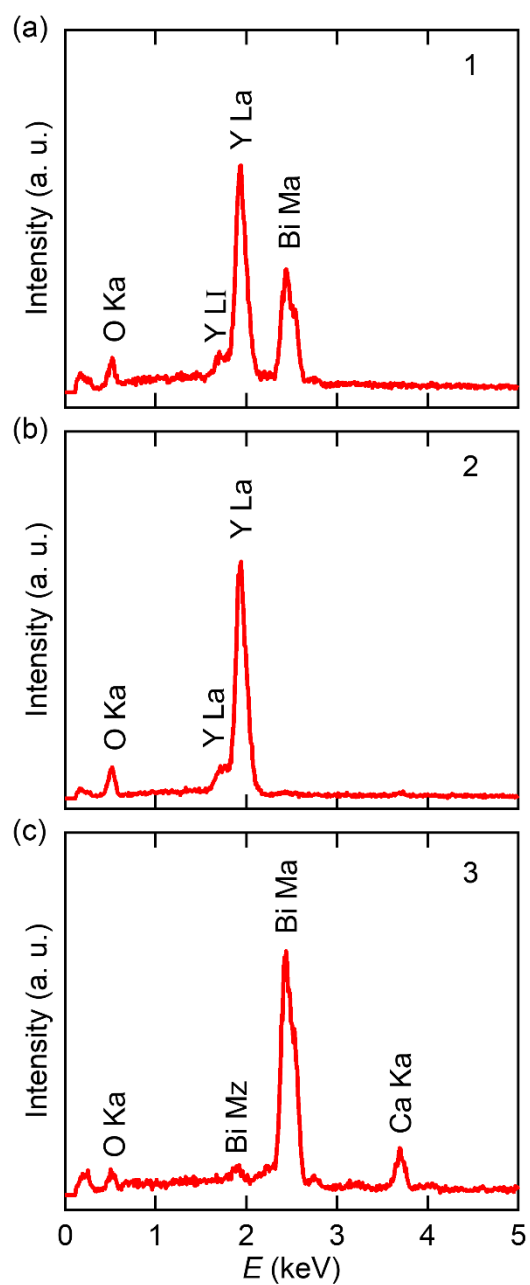


Figure S2. EDX spectrum of $Y_2(O,H)_2Bi$ ($x_H = 1.0$) measured at (a) area 1, (b) area 2, and (c) area 3 in Fig. S2a. The areas 1, 2, and 3 are considered to correspond to Y_2O_2Bi , Y_2O_3 , and Bi (mixed with Ca).

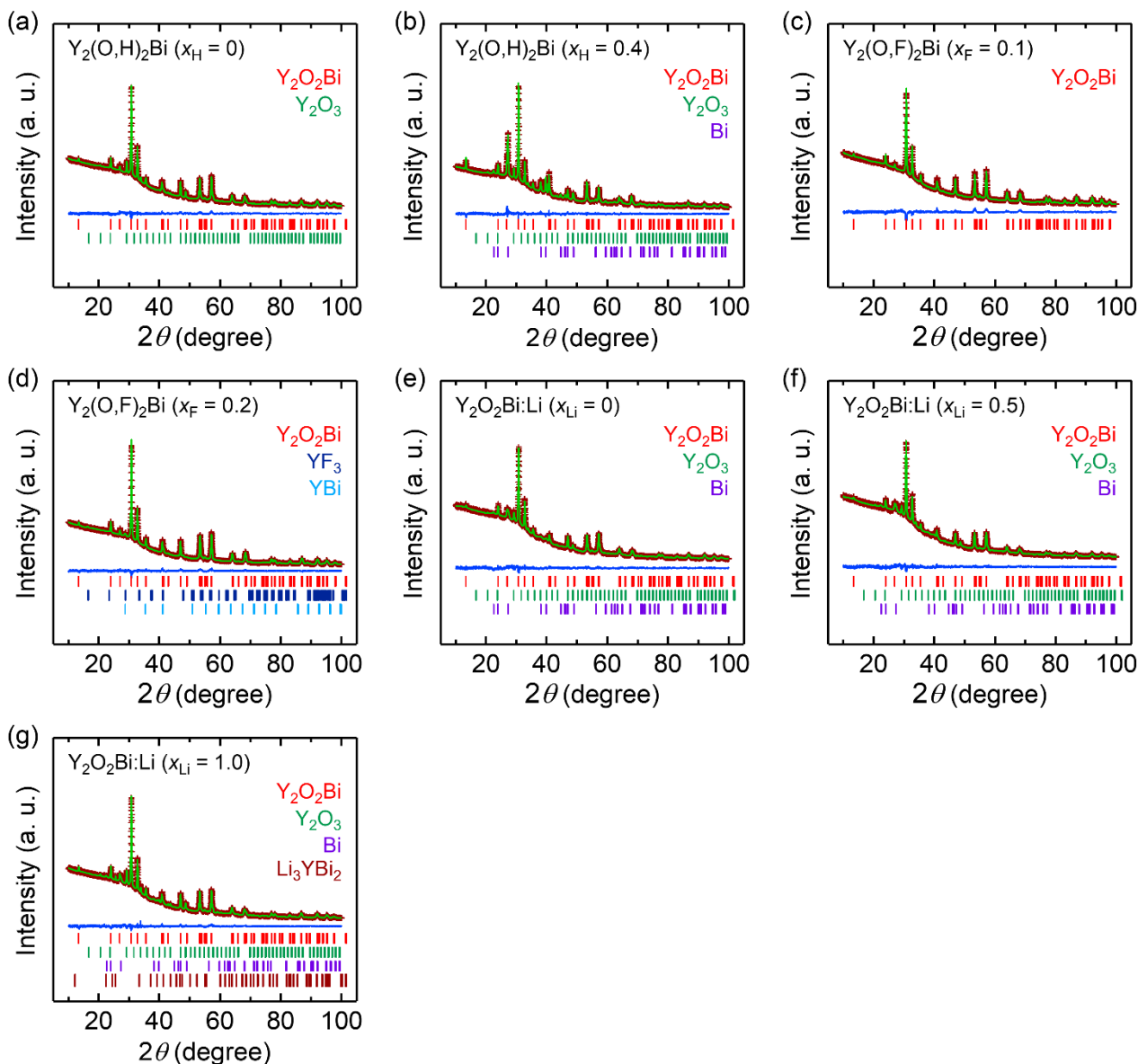


Figure S3 (a), (b) X-ray diffraction patterns and their Rietveld analysis for $Y_2(O,H)_2Bi$ ($x_H = 0, 0.4$, respectively). (c), (d) X-ray diffraction patterns and their Rietveld analysis for $Y_2(O,F)_2Bi$ ($x_F = 0.1, 0.2$). (e)–(g) X-ray diffraction patterns and their Rietveld analysis for $Y_2O_2Bi:Li$ ($x_{Li} = 0, 0.5, 1.0$), respectively.

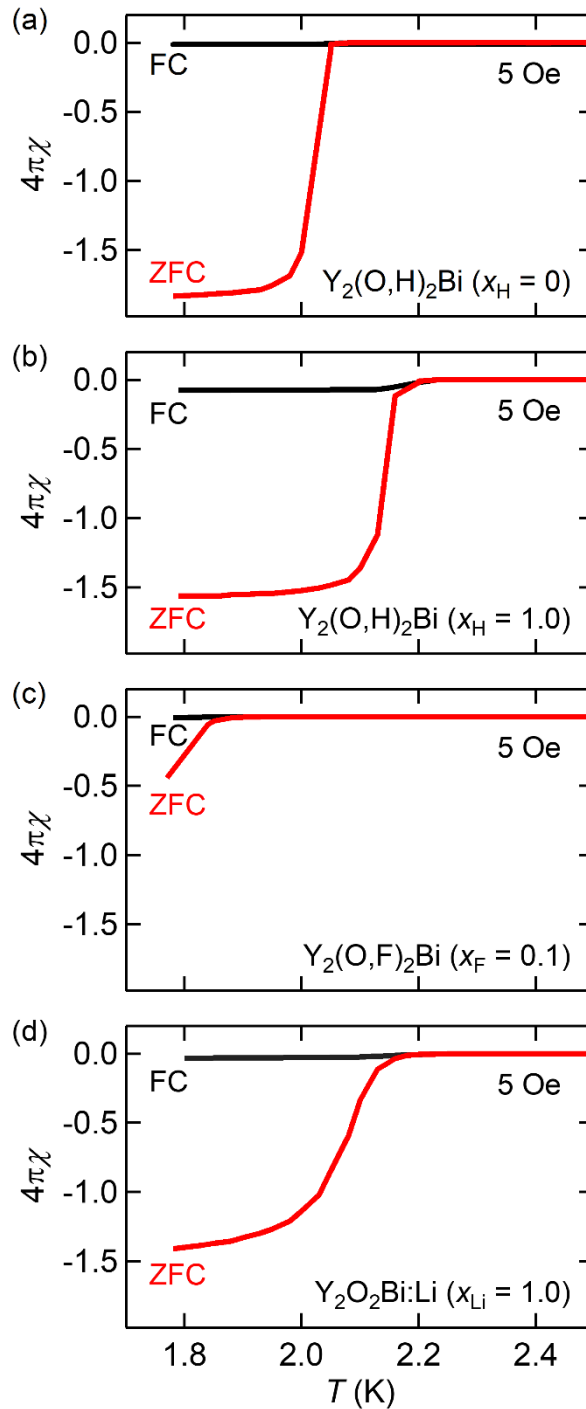


Figure S4 Temperature dependence of magnetic susceptibility for (a) $\text{Y}_2(\text{O,H})_2\text{Bi}$ ($x_{\text{H}} = 0$), (b) $\text{Y}_2(\text{O,H})_2\text{Bi}$ ($x_{\text{H}} = 1.0$), (c) $\text{Y}_2(\text{O,F})_2\text{Bi}$ ($x_{\text{F}} = 0.1$), and (d) $\text{Y}_2\text{O}_2\text{Bi}:\text{Li}$ ($x_{\text{Li}} = 1.0$). ZFC and FC represent zero field cooling and field cooling, respectively. It is noted that the superconducting volume fraction over unity was caused by using the theoretical density of $\text{Y}_2\text{O}_2\text{Bi}$ for the calculation.